Energy level decay processes in Ho3+-doped tellurite glass relevant to the 3-μm transition

# Energy level decay processes in $Ho^{3+}$-doped tellurite glass relevant to the 3 $\mu$m transition

Laércio Gomes,[1] Daniel Milanese,[2] Joris Lousteau,[2] Nadia Boetti,[2] and Stuart D. Jackson[3,a)]
[1]*Center for Lasers and Applications, IPEN/CNEN-SP, P.O. Box 11049, São Paulo, SP 05422-970, Brazil*
[2]*PhotonLab-DISMIC Politecnico di Torino, C.so Duca degli Abruzzi 24, 10129 Torino, Italy*
[3]*Institute of Photonics and Optical Science, School of Physics, University of Sydney, Camperdown, NSW 2006, Australia*

(Received 11 March 2011; accepted 7 April 2011; published online 17 May 2011)

The primary excited state decay processes relating to the $^5I_6 \rightarrow {}^5I_7 \sim 2.9$ $\mu$m laser transition in singly $Ho^{3+}$-doped tellurite (TZBG) glass have been investigated in detail using time-resolved fluorescence spectroscopy. Selective laser excitation of the $^5I_6$ energy level at 1151 nm and $^5I_7$ energy level at 1958 nm has established that the rate of energy transfer up-conversion between holmium ions excited to the $^5I_7$ level is negligible for $Ho^{3+}$ concentrations up to 4 mol. %. Excited state absorption was not observed from either the $^5I_7$ or $^5I_6$ levels and the luminescence from the $^5I_7$ and $^5I_6$ energy levels was measured to peak at ~2050 nm and ~2930 nm, respectively. The $^5I_6$ level has a low luminescence efficiency of ~8.9% due to strong nonradiative multiphonon relaxation. In contrast, decay from the $^5I_7$ level is essentially fully radiative. A linear decrease in the decay time of the $^5I_6$ level with $Ho^{3+}$ concentration augmentation results from energy transfer to $OH^-$ ions in the glass (with $N_{OH} \sim 8.2 \times 10^{17}$ ions $cm^{-3}$) and reduces the luminescence efficiency of the $^5I_6$ level to 8% for $[Ho^{3+}] = 4$ mol. %. Numerical simulation of a fiber laser incorporating 4 mol. % $Ho^{3+}$ showed that a population inversion of ~7.8% is reached for square pulses of 100 $\mu$s duration and a repetition frequency of 20 Hz at a moderate pump intensity of 418 kW $cm^{-2}$ if energy transfer to $OH^-$ radicals is neglected. © *2011 American Institute of Physics*. [doi:10.1063/1.3587476]

## I. INTRODUCTION

Rare earth doped fiber lasers developed for emission in the infrared wavelength region longer than 2 $\mu$m are of great interest for several applications, e.g., single frequency sources in this wavelength region would allow eye-safe coherent detection at long distance as a result of a number of atmospheric transmission windows that are available for $\lambda > 2$ $\mu$m. The efficient detection of various molecules would also be possible because they have strong vibrational absorption lines in this wavelength region, i.e., in the so-called molecular "fingerprint" region.[1,2] The use of the fiber geometry for the generation of shortwave and midwave infrared laser radiation introduces good thermal management and a comparatively low threshold because of the extended longitudinal dimension and small transverse cross section relevant to optical fibers.[3]

The $^5I_6 \rightarrow {}^5I_7$ and $^4I_{11/2} \rightarrow {}^4I_{13/2} \sim 3$ $\mu$m four-level transitions of $Ho^{3+}$ and $Er^{3+}$ offer broadband fluorescence and they have been successfully used to produce fiber lasers emitting in the shortwave infrared region in fluoride glasses.[4–6] The $Er^{3+}$ transition has received the most interest because fiber lasers based on this transition can be pumped with commercial diode lasers and an energy transfer up-conversion (ETU) process offers the potential for slope efficiencies beyond the Stokes limit. Pump excited state absorption (ESA) is strong, however, and may limit the maximum achievable output power as a result of thermal and photo-induced absorption losses.

The $Ho^{3+}$ ion, on the other hand, offers a longer free-running wavelength and little ESA, however, ETU cannot recycle the excitation and pump excitation is achieved with narrowly available diode lasers. Despite these limitations, the potential for high-power efficient operation of a ~3 $\mu$m fiber laser based on the $Ho^{3+}$ ion is strong and it is useful to study the characteristics of the $^5I_6 \rightarrow {}^5I_7$ transition of $Ho^{3+}$ when doped in robust materials that could allow for high-power pumping without the risk of optical or thermal damage. This investigation therefore involves a detailed spectroscopic study of $Ho_2O_3$-doped tellurite (TZBG) glasses with varying $Ho_2O_3$ concentrations. Tellurite glasses have received a lot of interest because of their low maximum phonon energy (of ~800 $cm^{-1}$) and robust thermomechanical properties. In the this study, we reveal the important radiative and nonradiative energy level decay processes that relate to the $^5I_6 \rightarrow {}^5I_7$ transition in tellurite glass after selective energy level excitation. Numerical simulations have been used to calculate the population inversion for the $^5I_6 \rightarrow {}^5I_7$ laser emission near 3 $\mu$m in a $Ho^{3+}$-doped (4 mol. %) tellurite (TZBG) glass fiber laser for cw pumping at 1153 nm.

## II. EXPERIMENTAL PROCEDURE

The $Ho^{3+}$-doped germanium tellurite (TZBG) glass samples used for the time-resolved luminescence spectroscopy were prepared from high-purity raw materials: 99.99% purity

a)Author to whom correspondence should be addressed. Electronic mail: s.jackson@usyd.edu.au.

 

$TeO_2$, $ZnF_2$, and $Bi_2O_3$; and 99.999% purity $GeO_2$. The glass composition was $(100-x)\times[74.5\ TeO_2\text{-}12.2\ ZnF_2\text{-}4.9\ Bi_2O_3\text{-}6.4\ GeO_2] + x\ Ho_2O_3$ with $x = 0.5$, 1, 2, and 4 mol. %. The starting powder materials were melted in a Pt-Au crucible in a dry glovebox environment at 900 °C for 30 min to reduce the $OH^-$ content in the glass. The molten liquids were poured into polished brass molds and annealed at 315 °C for 4 h to remove any mechanical stress. The glass density was 5.89 g $cm^{-3}$ and the measured refractive index was 1.98 at 2750 nm. The samples were cut and polished into $4.7\times10\times15$ $mm^3$ rectangular prisms. The $Ho^{3+}$ density was calculated to be $1.07\times10^{20}$ ions $cm^{-3}$, $2.14\times10^{20}$ ions $cm^{-3}$, $4.27\times10^{20}$ ions $cm^{-3}$ and $8.46\times10^{20}$ ions $cm^{-3}$ for the tellurite samples having $x = 0.5$, 1, 2, and 4 mol. %, respectively.

The absorption spectra in the range of 2000–10 000 nm were measured using a FTIR spectrophotometer. The decay characteristics of the excited states of $Ho^{3+}$ were measured using pulsed 10 mJ (4 ns) laser excitation from a tunable optical parametric oscillator (OPO) pumped by the second harmonic of a *Q*-switched Nd-YAG laser (Brilliant B from Quantel). Tunable laser excitation from the OPO was used to excite the $^5I_6$ energy level at 1151 nm and $^4I_7$ energy level at 1958 nm. The infrared luminescence (for $\lambda > 1000$ nm) was detected using an InSb infrared detector (Judson model J-10 D cooled to 77 K) in conjunction with a fast preamplifier with a response time of ~0.5 $\mu$s, and analyzed using a digital 200 MHz oscilloscope (Tektronix TDS 410). The visible and near infrared (i.e., $\lambda < 1100$ nm) was investigated using a photomultiplier tube (EMI) with a sensitive cathode of the S-1 or S-2 type (refrigerated to −20 °C); the photomultiplier has a response time of 20 ns. All the fluorescence decay characteristics were measured at 300 K. To isolate the infrared luminescence signals, bandpass filters each with ~80% transmission at 1200 nm or 2750 nm with a half width of 25 nm and an extinction coefficient of $\sim10^{-5}$ outside this band were used.

The optical absorption spectrum of $Ho^{3+}$ ions in tellurite glass has two main features in the near infrared, one feature at around 1958 nm from the $^5I_8 \rightarrow {}^5I_7$ transition and a second feature near 1151 nm due to $^5I_8 \rightarrow {}^5I_6$ transition. When the $Ho^{3+}$-doped material is excited at 1151 nm the following processes[7] are known to occur in fluoride glass:

(*a*) Ground state absorption (GSA); $Ho^{3+}\ (^5I_8) + h\nu\ (1151\ nm) \rightarrow Ho^{3+}\ (^5I_6)$

(*a'*) Excited state absorption (ESA); $Ho^{3+}\ (^5I_6) + h\nu\ (1151\ nm) \rightarrow Ho^{3+}\ (^5S_2)$

(*b*) Energy transfer up-conversion (ETU1); $Ho^{3+}\ (^5I_7) + Ho^{3+}\ (^5I_7) \rightarrow Ho^{3+}\ (^5I_6) + Ho^{3+}\ (^5I_8)$

(*b'*) Energy transfer up-conversion (ETU2); $Ho^{3+}\ (^5I_6) + Ho^{3+}\ (^5I_6) \rightarrow Ho^{3+}\ (^5F_5) + Ho^{3+}\ (^5I_8)$

(*c*) Cross-relaxation (CR); $Ho^{3+}\ (^5S_2) + Ho^{3+}\ (^5I_8) \rightarrow Ho^{3+}\ (^5I_4) + Ho^{3+}(^5I_7)$

Each of the processes listed above has been shown to affect the operation of the the 3 $\mu$m laser in the cw pumping regime in $Ho^{3+}$-doped ZBLAN glass.[7]

## III. EXPERIMENTAL RESULTS

Figure 1 shows the visible to shortwave (a) and midwave (b) absorption spectra of $Ho^{3+}$ (2 mol. %)-doped tellurite glass. The spectrum shows a broad strong absorption band between 2500 $cm^{-1}$ and 3500 $cm^{-1}$, which we attribute to free $OH^-$ groups.[8] The narrow absorption band due to isolated $OH^-$ radicals, with maximum absorption at ~3735 $cm^{-1}$, was not observed. The concentration of $OH^-$ radicals is given by $N_{OH} = \frac{N_{Av}\alpha}{\xi}$, where $N_{Av}$ is Avogadro's constant $(6.02\times10^{23})$, $\alpha$ is the absorption coefficient (=0.0672 $cm^{-1}$, relevant to the $OH^-$ vibration band at 3085 $cm^{-1}$), and $\xi$ is the absorptivity of free $OH^-$ groups in the glass. Using $\xi = 49.1\times10^3$ $cm^2$ $mol^{-1}$ (Ref. 9), we estimated the $OH^-$ concentration in our samples to be $8.24\times10^{17}$ ions $cm^{-3}$; a value ~29 times smaller than the free $OH^-$ density (of $2.4\times10^{19}$ $cm^{-3}$) found in $Er^{3+}$-doped germanotellurite glass produced from drying the melt using oxygen gas and $CCl_4$ bubbling.[10]

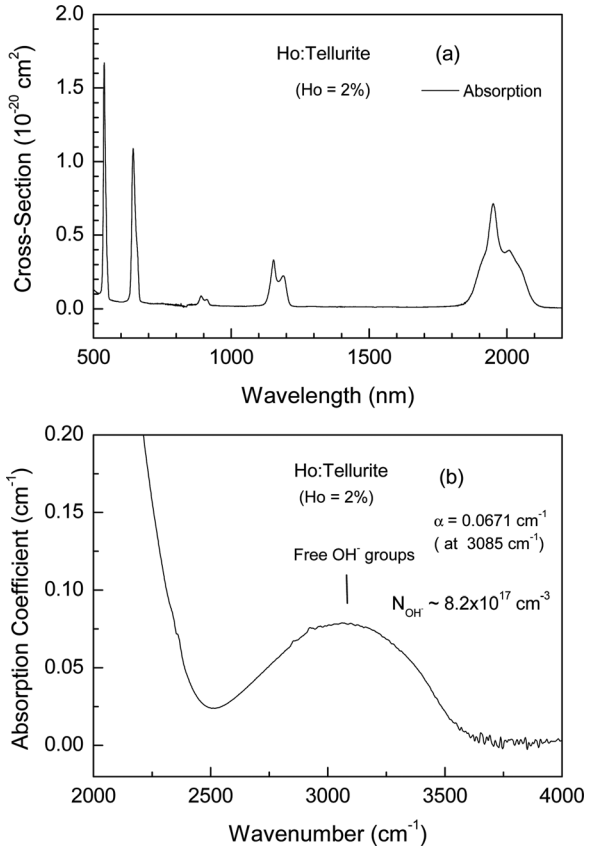


FIG. 1. Measured absorption transitions in the (a) visible and shortwave infrared region and (b) $OH^-$ vibration feature in $Ho^{3+}$(2 mol. %)-doped TZBG glass (sample thickness = 4.7 mm).

### A. Infrared fluorescence spectrum of $Ho^{3+}$ in tellurite (TZBG) glass

The fluorescence emission spectrum of $Ho^{3+}$ in the shortwave infrared was measured for $[Ho^{3+}] = 4$ mol. %. Figure 2 shows that there are two emission bands; one from the $^5I_6$ level at ~2930 nm and one from the $^5I_7$ level at ~2050 nm. The emission cross section due to $^5I_6 \rightarrow {}^5I_7$ and $^5I_7 \rightarrow {}^5I_8$ transitions was calculated using $\sigma_{emis}(\lambda) = \frac{\bar{\lambda}^4}{8\pi n^2 c} A_{ij} \frac{S(\lambda)}{\int S(\lambda)d\lambda}$, where $\bar{\lambda}$ is the average emission wavelength or centroid, $A_{ij}$

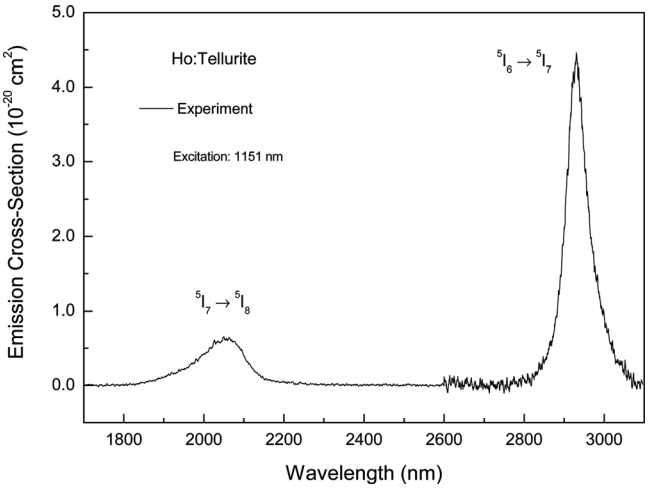


FIG. 2. Measured emission spectrum of $Ho^{3+}$(4 mol. %)-doped tellurite (TZBG) glass using a pulsed laser excitation at 1151 nm with an average energy of 13 mJ and pulse duration of 4 ns. Spectrum was measured using a boxcar technique.

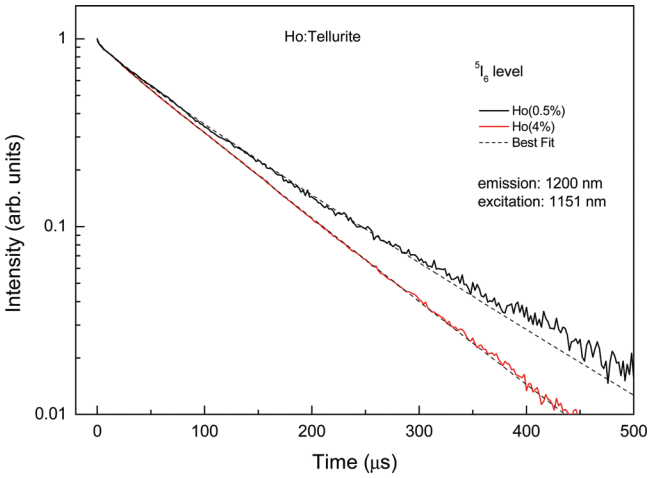


FIG. 3. (Color online) Measured emission decay characteristic (solid lines) of the $^5I_6$ level of $Ho^{3+}$ (0.5 and 4 mol. %)-doped tellurite (TZBG) glass using short pulse laser excitation at 1151 nm with an average energy of 10 mJ and pulse duration of 4 ns at 10 Hz. Broken lines indicate the best fit using the Burshtein model of Eq. (1).

($s^{-1}$) is the radiative transition probability, S($\lambda$) is the line shape of the emission band, $\int S(\lambda)d\lambda$ is the integrated line shape, $n$ is the refractive index (= 1.98), and $c$ is the speed of light.

The emission cross section of the $^5I_6 \rightarrow {}^5I_7$ transition was calculated using the radiative transition probability $A_{ij} = 138\ s^{-1}$,[11] the experimental value of $\overline{\lambda} = 2930$ nm, and $S(\overline{\lambda})/\int S(\lambda)d\lambda = 1.25 \times 10^{-2} nm^{-1}$, which gave an emission cross section of $4.30 \times 10^{-20}$ cm$^2$ at the maximum emission wavelength of 2930 nm. The emission cross section of the $^5I_7 \rightarrow {}^5I_8$ transition was calculated using the radiative transition probability $A_{ij} = 1/\tau_R$ (where $\tau_R = 5.8$ ms calculated below), the experimental value of $\overline{\lambda} = 2050$ nm and $S(\overline{\lambda})/\int S(\lambda)d\lambda = 6.16 \times 10^{-3} nm^{-1}$, which provides an emission cross section of $6.37 \times 10^{-21}$ cm$^2$ at 2050 nm. The radiative lifetime of the $^5I_7$ level was calculated according to the relationship[12] $\tau_{rad} = \frac{(2J+1)}{(2J'+1)} \frac{\overline{\lambda}^4}{8\pi c n^2 \int \sigma_{abs}(\lambda)d\lambda}$, where $\tau_{rad}$ is the radiative lifetime, J and J′ the total momentum for the upper and lower levels, $\int \sigma_{abs}(\lambda)d\lambda$ is the integrated absorption cross section of the 2 $\mu$m band, and $\overline{\lambda}$ the mean wavelength of the absorption band. The radiative lifetime of the $^5I_7$ level was calculated using the $\overline{\lambda} = 1964$ nm and the integrated absorption cross section $\int \sigma_{abs}(\lambda)d\lambda = 7.7016 \times 10^{-26} cm^3$ obtained from the spectrum shown in Fig. 1(a), giving $\tau_{rad} = 5.8$ ms, which is longer than the 3.52 ms for this lifetime given in Ref. 11.

### B. Emission decay from the $^5I_6$ level

Figure 3 shows the emission decay characteristic at 1200 nm for $[Ho^{3+}] = 0.5$ and 2 mol. % after laser excitation at 1151 nm with a mean pulse energy of 10 mJ and 4 ns pulse duration. The luminescence decay of $^5I_6$ excited state was nonexponential and was fitted using the Burshtein model,[13]

$$I(t) = I_0 \exp(-\gamma\sqrt{t} - t/\tau_m), \quad (1)$$

where $\gamma$ ($s^{-1/2}$) is the transfer constant due to the direct donor to acceptor transfer and $\tau_m$ is defined by

$$1/\tau_m = 1/\tau_R + W_{nR} + \omega, \quad (2)$$

where $\tau_R$ is the radiative lifetime and $\omega$ is the transfer constant ($s^{-1}$) due to the migration assisted donor to acceptor transfer. $W_{nR}$ is the nonradiative multiphonon decay rate ($s^{-1}$). Because the luminescence decay of $^5I_6$ level at 1200 nm was nonexponential, the effective $^5I_6$ lifetime ($\tau$) was obtained by integration,[14] according to

$$\tau = \frac{1}{I_0}\int_0^\infty I(t)dt, \quad (3)$$

The best fit to the measured 1200 nm luminescence decay curve was carried out using Eq. (1); see dotted line in Fig. 3. The fitting parameters were: (i) $\gamma = 32.4\ s^{-1/2}$, $\tau_m = 136.8$ $\mu$s, and $\tau = 99.2$ $\mu$s for $[Ho^{3+}] = 0.5$ mol. % ($R^2 = 0.997$); (ii) $\gamma = 28\ s^{-1/2}$, $\tau_m = 126$ $\mu$s, and $\tau = 96.3$ $\mu$s for $[Ho^{3+}] = 1$ mol. % ($R^2 = 0.999$); (iii) $\gamma = 23.4\ s^{-1/2}$, $\tau_m = 119.3$ $\mu$s, and $\tau = 95.7$ $\mu$s for $[Ho^{3+}] = 2$ mol% ($R^2 = 0.999$); and (iv) $\gamma = 14.8\ s^{-1/2}$, $\tau_m = 102.1$ $\mu$s, and $\tau = 89.6$ $\mu$s for $[Ho^{3+}] = 4$ mol. % ($R^2 = 0.999$).

Figure 4(a) shows that the decay time measured for $^5I_6$ level is linearly dependent on the $Ho^{3+}$ concentration in tellurite (TZBG) glass. This effect was attributed to energy transfer from the $^5I_6$ level to $OH^-$ radicals (i.e., free $OH^-$ groups) that are present in the samples with the estimated concentration of $8.24 \times 10^{17}$ ions cm$^{-3}$. The rate of energy transfer to the radicals was obtained using

$$W_t = 1/\tau - 1/\tau_R - W_{nR}. \quad (4)$$

The intrinsic lifetime ($\tau_d$) of the $^5I_6$ level was obtained by extrapolating the line in Fig. 4(a) to $[Ho^{3+}] = 0$, which gave $\tau_d = 100$ $\mu$s. Assuming that for very low $Ho^{3+}$ concentration, $W_t$ is negligible and $\tau_R = 1.12$ ms (Ref. 11) we obtain a value for the nonradiative decay rate, $W_{nR} = 9107\ s^{-1}$ for the $^5I_6$ level. The following values of $W_t$ were obtained: (i) 76.6 $s^{-1}$ ($[Ho^{3+}] = 0.5\%$), (ii) 379 $s^{-1}$ ($[Ho^{3+}] = 1\%$), (iii) 445 $s^{-1}$

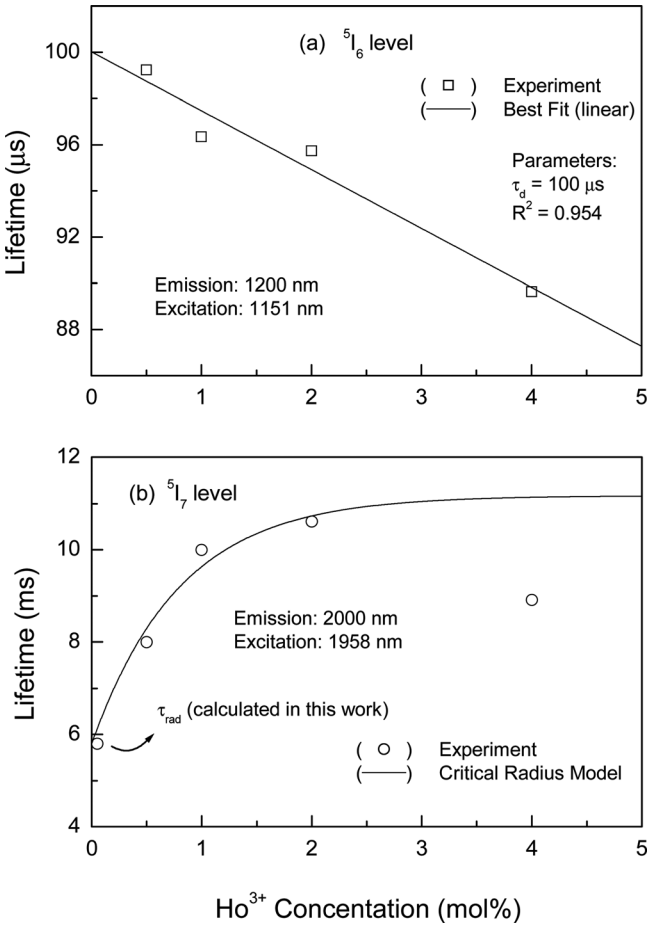


FIG. 4. Measured decay time ($\tau$) of (a) $^5I_6$ level measured at 1200 nm using laser excitation at 1151 nm (E = 10 mJ, 4 ns) and (b) $^5I_7$ level measured for the luminescence decay at 2000 nm using the laser excitation at 1958 nm (E = 10 mJ, 4 ns) for $Ho^{3+}$-doped TZBG glass as a function of [$Ho^{3+}$]. The solid line in (b) represents the best fit using the critical radius model given by Eq. (5), where $\tau_{rad}$ = 5.8 ms, and the fitting parameters are $\tau_0$ = 5.3 ms and $N_C$ = 0.8 mol. %.

([$Ho^{3+}$] = 2%), and (iv) 1157 $s^{-1}$ ([$Ho^{3+}$] = 4%). These values for $W_t$ are essentially linearly dependent on [$Ho^{3+}$] and indicate that $^5I_6$ energy level migration is important. As a consequence of energy transfer to $OH^-$, the luminescence efficiency from $^5I_6$ level decreases from 8.9 to 8% for [$Ho^{3+}$] = 4%. From these calculations it is clear that the main decay process for the $^5I_6$ level is multiphonon decay.

### C. Emission decay from the $^5I_7$ level

Figure 5 shows the emission decay from the $^5I_7$ level measured at 2000 nm by pulsed laser excitation at 1958 nm (E = 10 mJ). The emission decay from the $^5I_7$ state is observed to be exponential (see broken lines in Fig. 5), which indicates weak energy transfer to free $OH^-$ radicals. It can be observed from Fig. 4(b) that the $^5I_7$ decay time initially increases with increasing $Ho^{3+}$ concentration up to [Ho] ~ 2% and displays a slight decrease to [Ho] = 4%. The measured decay times for the $^5I_7$ level are longer than the calculated radiative lifetime ($\tau_R$ = 5.8 ms, calculated above). The increase level in the decay time of the $^5I_7$ in our experiment relates to strong excitation migration from a nonradiative resonant dipole-dipole interaction between the $^5I_7$ and $^5I_8$ energy levels. This phenomenon explains the initial increase in the decay time as the $Ho^{3+}$ concentration is increased. Note that measuring the luminescence close to the pumped surface can minimize radiation trapping. In our experiment, we observed an increase in the decay time at distances perpendicular to the pump of ~8 mm, however, for distances of ~3 mm and shorter (from where we took the measurements) the measured decay time was invariable.

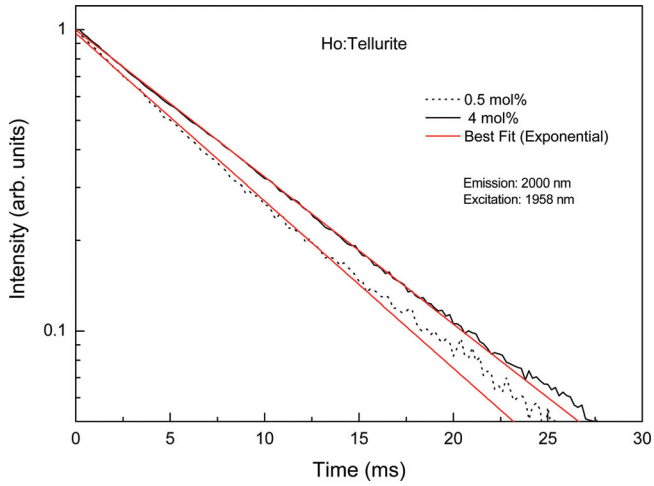


FIG. 5. (Color online) Measured emission decay characteristics (solid lines) of the $^5I_7$ level of $Ho^{3+}$(0.5 and 4 mol. %)-doped TZBG glass using a short pulse laser excitation at 1958 nm with an average energy of 10 mJ and pulse duration of 4 ns at 10 Hz. Broken lines represent the best fit using an exponential decay model.

The line of best fit to the decay time characteristic [open circles in Fig. 4(b)] with the increase in [$Ho^{3+}$] was carried out using Eq. (5). Equation (5) predicted that the lifetime of the $^5I_7$ level increases if a $Ho^{3+}$ ion excited to the $^5I_7$ level will transfer excitation to a ground state $Ho^{3+}$ ion within a critical distance, $R_C$, with a decay time augmentation efficiency, $\eta(\tau)$, dependent on the $Ho^{3+}$ concentration.[15,16] This model predicts a saturation of the decay time increase to a value ($\tau_R + \tau_0$), which should be reached for $N_{Ho} > N_C$, where $N_C$ is the critical concentration calculated from

$$\eta(Ho) = 1 - \exp(-N_{Ho}/N_C) \quad \tau_d = \tau_R + \eta(Ho)\tau_0 \qquad (5)$$

where $\tau_R$ = 5.8 ms and $N_{Ho}$ is the $Ho^{3+}$ concentration. The best fit using Eq. (4) gives $\tau_0$ = 5.3 ms and $N_C$ = 0.8 mol. % [see solid line in Fig. 4(b)].

No up-conversion processes (ESA or ETU) starting from the $^5I_7$ or $^5I_6$ levels were observed in our measurements. The expected green emission from the $^5S_2$ level or the red emission from the $^5F_5$ level was not observed despite that the fact that it can be easily observed in $Ho^{3+}$-doped ZBLAN glass under pulsed laser excitation at 1958 nm (Ref. 16) or in $Er^{3+}$-doped tellurite glass with 980 nm pumping.[21]

## IV. DISCUSSION

Tellurite glasses are an interesting alternative host material for shortwave and midwave infrared fiber lasers; because they combine a relatively low phonon energy with higher

thermal and chemical stability compared with, for example, fluoride glasses. On the other hand, tellurite glasses display lower luminescence efficiencies compared to fluoride glasses but they display higher emission cross sections and are easier to handle and splice to silica fibers. Tellurite glasses have shown efficient emission at $\sim 2$ $\mu$m from $Tm^{3+}$, $Ho^{3+}$-co-doped tellurite glass optical fiber lasers;[17–19] however, there has been no demonstration of laser operation beyond $\sim 2$ $\mu$m in tellurite glass.

The results presented here indicate that perhaps the main issue with these glasses are water incorporation and the low luminescence efficiency of the $^5I_6$ level. To illustrate this we have carried out a numerical simulation to predict the performance of $Ho^{3+}$-doped tellurite fiber lasers. The experimental observation that ETU1 is weak in $Ho^{3+}$-doped TZBG glass (at least up to $[Ho^{3+}] = 4$ mol. %) implies that unlike the $Er^{3+}$-doped ZBLAN system,[20] energy recycling is not possible for moderately concentrated $Ho^{3+}$-doped tellurite glasses when pumped into the $^5I_6$ level.

The rate equations were written to include the essential energy levels and pump and decay processes for laser emission at 2930 nm when the $^5I_6$ level is excited with pump radiation. The rate equations are

$$\frac{dn_1}{dt} = -R_P n_1 + \frac{n_2}{\tau_2} + \frac{\beta_{31}}{\tau_{R3}} n_3, \tag{6}$$

$$\frac{dn_2}{dt} = -\frac{n_2}{\tau_2} + \frac{\beta_{32}}{\tau_{R3}} n_3 + W_{nR}(32) n_3 + W_t(2) n_3, \tag{7}$$

$$\frac{dn_3}{dt} = R_P n_1 - \frac{n_3}{\tau_{R3}} - W_{nR}(32) n_3 - W_t(2) n_3, \tag{8}$$

where $n_1$, $n_2$, and $n_3$ indicate the $^5I_8$, $^5I_7$, and $^5I_6$ levels and $n_1 + n_2 + n_3 = x$, where $x = 0.005$, 0.01, 0.02, and 0.04 (i.e., mole fraction). The radiative lifetimes, luminescence branching ratios, and nonradiative multiphonon decay rate values that were obtained from our experiment are: $\tau_{R3} = 1.12$ ms, $\beta_{32} = 0.16$, $\beta_{31} = 0.84$, $\tau_2 = 8.9$ ms (4 mol. %), $W_{nR}(32) = 9107$ $s^{-1}$, and $W_t(2) = 1157$ $s^{-1}$. Note that $W_{nR}(21) \sim 0$. The pump rate ($R_P$) can be converted to pump irradiance ($I_P$) using the relation: $R_P(s^{-1}) = \frac{\sigma_{abs}(\lambda)}{h\nu} I_P(\mathrm{Wcm}^{-2})$. Using the absorption cross section $\sigma_{abs}(\lambda) = 3.3 \times 10^{-21}$ $cm^2$ for the pump wavelength $\lambda = 1153$ nm, one obtains $R_P = 1000$ $s^{-1}$ for a pump intensity $I_P = 52.2$ kW $cm^{-2}$.

The calculated evolution of the excited state populations $n_3$ and $n_2$ (in $cm^{-3}$) were used to determine the population difference ($n_3 - n_2$), as shown in Fig. 6. One can see that steady state is reached in a time <2 ms. At equilibrium, the populations $n_1$, $n_2$, and $n_3$ were used to calculate the population inversion $\Delta n = n_3 - n_2$ for $[Ho^{3+}] = 0.5$, 1, 2, and 4 mol. % for a number of pump intensities at 1153 nm. For all the simulations, we obtained a steady state but negative population inversion [even with $W_t(2) = 0$]. A positive population inversion, however, occurs for pump times shorter than 100 $\mu$s with a maximum in $\Delta n$ occurring 55 $\mu$s after the pump is switched on; see Fig. 7(a). This result indicates that maximum laser emission can be achieved by pump pulses of 55 $\mu$s duration with a minimal interval of time between pulses of 50 ms. [This time interval is necessary for complete emptying of the $^5I_7$ level, as shown in Fig. 7(b)]. Using a square modulated 50 $\mu$s duration pump one can get $\Delta n = 0.75$ mol. % for $[Ho^{3+}] = 4$ mol. %.

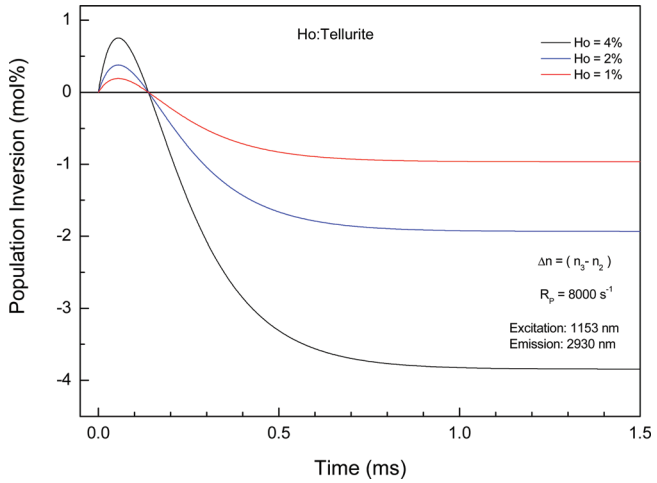


FIG. 6. (Color online) Calculated population inversion ($n_3 - n_2$) for cw pumping of $Ho^{3+}$-doped TZBG glass using a pumping intensity of $\sim 418$ kW $cm^{-2}$ ($R_p = 8000$ $s^{-1}$) for $[Ho^{3+}] = 1$, 2, and 4 mol. %.

Figure 8 shows the maximum calculated population inversion using square 1153 nm pump pulses of varying

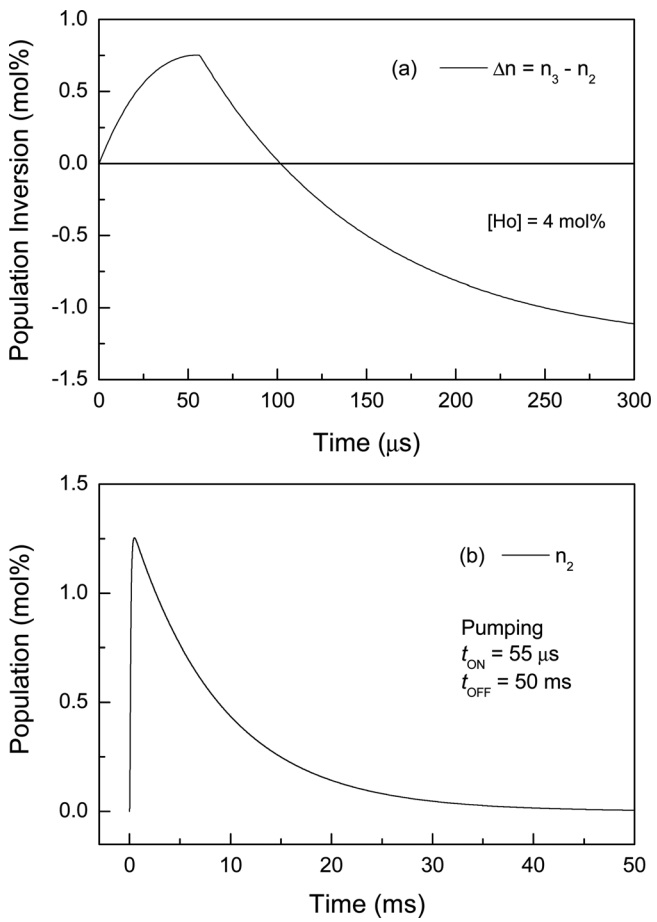


FIG. 7. Calculated (a) population inversion ($n_3 - n_2$) for a square pump pulse of 55 $\mu$s duration and pulse period= 50 ms and (b) $^5I_7$ population ($n_2$). The pump intensity was 418 kW $cm^{-2}$ at 1153 nm, $[Ho^{3+}] = 4$ mol. %, $W_t = 0$.

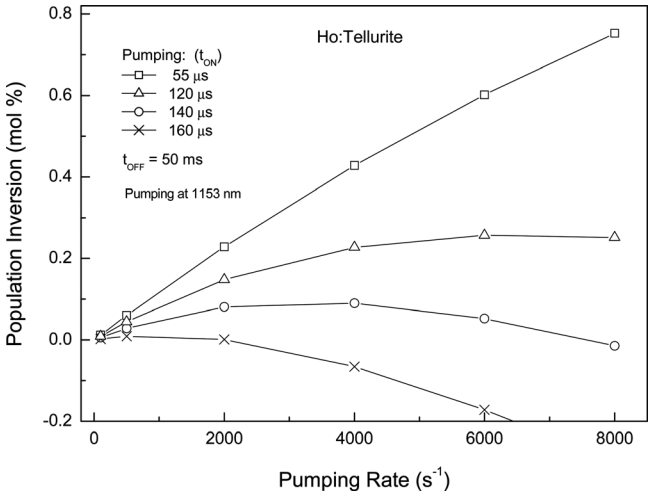


FIG. 8. Calculated population inversion for a square pump pulse for several pulse durations and a fixed interpulse period of 50 ms for $Ho^{3+}$(4 mol. %)-doped TZBG glass as a function of the pump rate ($R_P$).

duration for $[Ho^{3+}] = 4$ mol. % as a function of the pump rate ($R_P$). It can be observed that the population inversion is greatest when $t_{ON} = 55$ $\mu$s and the population inversion decreases with increasing pumping duration. Note that for these simulations, no losses were included and, hence, the simulations are only a guide to possible performance from a fiber laser arrangement.

## V. SUMMARY AND CONCLUSIONS

The decay processes relating to the $^5I_7 \rightarrow {}^5I_8 \sim 2$ $\mu$m and $^5I_6 \rightarrow {}^5I_7 \sim 2.9$ $\mu$m laser transitions in singly $Ho^{3+}$-doped tellurite (TZBG) glass were investigated in detail using selective laser excitation of the $^5I_6$ energy level at 1151 nm and $^5I_7$ energy level at 1958 nm. The results have established that a nonradiative ETU between two excited $Ho^{3+}$ ions in the $^5I_7$ level is negligibly weak for $Ho^{3+}$ concentrations $\leq$4 mol. %. Pump ESA from the $^5I_7$ or $^5I_6$ levels was not observed when these levels were excited directly. The $^5I_7$ and $^5I_6$ energy levels were measured to emit luminescence with peaks at $\sim$2050 nm and $\sim$2930 nm, respectively. The $^5I_6$ level has low luminescence efficiency of 8% because of nonradiative multiphonon relaxation, however, decay from the $^5I_7$ level was observed to be fully radiative. The decreasing decay time of the $^5I_6$ level with increasing $[Ho^{3+}]$ was attributed to energy transfer to the $OH^-$ radicals present in the glass. The numerical simulations indicate that the prospect for cw operation on the $^5I_6 \rightarrow {}^5I_7$ transition is low in $Ho^{3+}$-doped tellurite glass.

## ACKNOWLEDGMENTS

The authors gratefully acknowledge financial support from the Australian Research Council. One of the authors (L. Gomes) thanks FAPESP (Grants Nos. 1995/4166-0 and 2000/10986-0) and CNPq for financial support. The effort to produce Ho-doped tellurite glass samples of high purity and low $OH^-$ content was sponsored by the Air Force Office of Scientific Research (USAFOSR), Air Force Material Command, USAF, under grant number FA8655-09-1-3111.

[1]A. Schliesser, M. Brehm, F. Keilmann, and D. W. van der Weide, Opt. Express **13**, 9029 (2005).
[2]M. Brehm, T. Taubner, R. Hillenbrand, and F. Keilmann, Nano Lett. **6**, 1307 (2006).
[3]M. Pollnau and S. D. Jackson, "Mid-infrared fiber lasers" in *Solid-state mid-infrared laser sources* (Springer-Verlag, Berlin, 2003) p. 225-261.
[4]S. D. Jackson, T. A. King, and M. Pollnau, Opt. Lett. **24**, 1133 (1999)
[5]S. Tokita, M. Murakami, S. Shimizu, M. Hashida, and S. Sakabe, Opt. Lett. **34**, 3062 (2009).
[6]S. D. Jackson, Opt. Lett. **29**, 334 (2004).
[7]A. F. H. Librantz, S. D. Jackson, L. Gomes, S. J. L. Ribeiro, and Y. Messaddeq, J. Appl. Phys. **103**, 023105 (2008).
[8]M. Arnaudov, Y. Dimitriev, V. Dimitrov, M. DimitrovapankovaI, Phys. Chem. Glasses **27**, 48 (1986)
[9]L. Nemec and J. Gotz, J. Am. Ceram. Soc. **53**, 526 (1970).
[10]X. Feng, S. Tanabe, and T. Hanada, J. Non-Cryst. Solids **281**, 48 (2001)
[11]A. K. Singh, S. B. Rai, and V. B. Singh, J. Alloys Compd. **403**, 97 (2003).
[12]X. Zou and H. Toratani, Phys. Rev. B **52**, 15889 (1995)
[13]A. I. Burshtein, Sov. Phys. JEPT **35**, 882 (1972).
[14]A. Braud, S. Girard, D. L. Doualan, M. Thuau, R. Moncorge, and A. M. Tkachuk, Phys. Rev. B **61**, 5280 (2000).
[15]L. Gomes, A. F. H. Librantz, F. H. Jagosich, W. A. L. Alves, I. M. Ranieri, and S. L. Baldochi, J. Appl. Phys. **106**, 103508 (2009).
[16]A. F. H. Librantz, S. D. Jackson, S. D. F. H. Jagosich, L. Gomes, G. Poirier, S. J. L. Ribeiro, and Y. Messaddeq, J. Appl. Phys. **101**, 123111 (2007).
[17]J. S. Wang, E. Snitzer, E. M. Vogel, and G. H. Sigel Jr., J. Lumin. **60–61**, 145 (1994).
[18]B. Richards, A. Jha; Y. Tsang, D. Binks, Lousteau, J. F. Fusari, A. Lagatsky, C. Brown, and W. Sibbett, Laser Phys. Lett. **7**, 177 (2010)
[19]Y. Tsang, B. Richards, D. Binks, J. Lousteau, and A. Jha, Opt. Lett. **33**, 1282 (2008)
[20]M. Pollnau, S. D. Jackson, IEEE J. Quantum Electron. **38**, 162 (2002).
[21]L. Gomes, M. Oermann, H. Ebendorff-Heidepriem, D. Ottaway, T. Monro, A. Felipe, H. Librantz, S. D. Jackson, "Energy level decay and excited state absorption processes in erbium-doped tellurite glass," J. Appl. Phys. (submitted)